Analysis on Multipath Shape Factors of Air-to-Ground Radio Communication Channels

Sardar Muhammad Gulfam*, Syed Junaid Nawaz*, Abrar Ahmed*, and Mohammad N. Patwary+.

*Department of Electrical Engineering, COMSATS Institute of Information Technology, Islamabad, Pakistan.
+Faculty of Computing, Engineering, and Sciences, Staffordshire University, Stafford, UK.
sardar_muhammad@comsats.edu.pk, *junaidnawaz@ieee.org*,
abrar_ahmed@comsats.edu.pk,
and *m.n.patwary@staffs.ac.uk*

Abstract

This paper first presents an extension of a notable three dimensional (3D) channel model for air-to-ground (A2G) radio propagation environments, from the plain distribution of angular energy to its quantization in terms of multipath shape factors (SFs). Next, the paper presents a comprehensive analysis on the characteristics of multipath SFs for A2G radio propagation environments observed at both ends of the link. The analysis include the impact of various physical channel parameters on angular spread, true standard deviation, angular constriction, and direction of maximum fading. These SFs are obtained by exploiting the analytical and empirical results available in the literature for the distribution of energy in 3D angular space. Finally, a mechanism for classification of A2G propagation environments into taxiing, en-route, and take-off scenarios on the basis of SFs is presented.

Keywords: Angle of Arrival, Multipath shape factors, Angular spread, Air-to-ground, Standard Deviation, Angular Constriction.

I. Introduction

The technologies of communication for air-to-ground (A2G) and ground-to-air (G2A) have evolved with time. In early days, color paddles, hand signals and other visual aids were used for A2G/G2A communications. Technology developments improved these methods by the use of wireless telegraphy and A2G radio systems. In today's world of communication when researchers are implementing 5th generation (5G) wireless communication systems for providing high speed and reliable network global coverage, the internet access in aircrafts is now at the high demand. A reliable communication link is required to provide high speed data services to the passengers as well as for navigation and security services to the airplanes. It is expected in future for dramatic increase in the use of unmanned air vehicle (UAV) for purposes like military applications, cargo delivery, industrial inspection, weather monitoring, emergency humanitarian missions, and remote sensing. A reliable A2G link for such UAV communication nodes is also of immense importance. It is of high importance to have accurate knowledge of channel statistics at both

the communicating ends for establishing a reliable communication link. The rapid fluctuations in received signals in a multipath channel are termed as small-scale fading [1]. In the literature, first-order channel statistics are analyzed through characterization of small-scale fading with probability density functions (PDFs) of angle of arrival (AoA). However, Durgin $et\ al.$ has strengthened the theory of small-scale fading by deriving a new concept of multipath shape factors (SFs) in [2]. Durgin $et\ al.$ derived three SFs which are the angular spread, the angular constriction, and the direction of maximum fading by using PDF of AoA. In [3], these three SFs are redefined on the basis of trigonometric moments and a new quantifier, named true standard deviation, is proposed. Applications of these SFs in Nakagami-m fading channels is discussed in [4, 5]. Various intensive studies on AoA, time of arrival (ToA) and Doppler spectrum analysis for land-mobile radio cellular communication channels has been proposed in the literature [6–10]. The analysis on SFs for such land mobile communication environments assuming both geometric channel models and measurement based models is presented in [11–13]. The multipath SFs are core parameters in studying second order fading statistics of the channel including level crossing rate, average fade duration, auto-covariance and coherence distance [7]. No such study on the SFs of A2G communication scenarios has been conducted in the literature. Various A2G communication scenarios lead to a rich multipath fading environment [14–16]. Therefore, it becomes imperative to conduct a thorough study on SFs for A2G communication environments and to analyze the impact of physical channel's parameters on these SFs.

In this paper, an extension of a notable three dimensional (3D) analytical model [17] for aeronautical communication channels is presented from the plain distribution of angular energy to the quantization of multipath SFs. The multipath AoA distributions for A2G/G2A communication environment are characterized by using the multipath SFs: the angular spread, the standard deviation, the angular constriction, and the angle of maximum fading. These SFs are computed by using PDF of AoA observed at both end of aeronautical communication link with respect to azimuth and elevation planes with the approach used in [2, 3, 11–13]. The effects of different physical parameters of the proposed model on SFs is also been observed. The rest of this paper is organized as follows: Section II discusses the proposed methodology and system model. Discussion on obtained simulation results is given in Section III. Finally, the conclusions on obtained analytical results are made in section IV.

II. Proposed Methodology and System Model

Aeronautical communication environment is such a scenario in which airplane communicates with their ground base station (BS). The block diagram of such scenario is given in Fig. 1. Air station (AS) is assumed

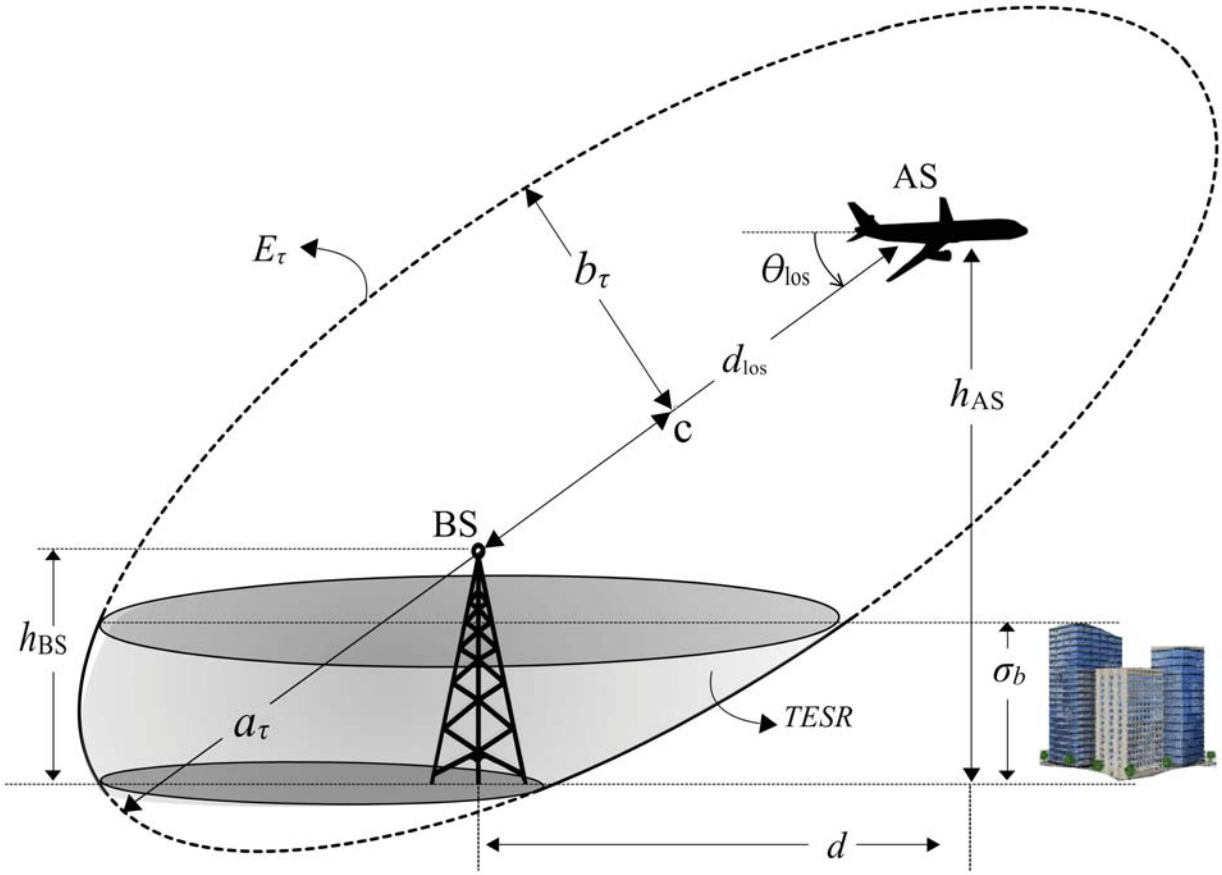

Fig. 1. Aeronautical communication environment.

at an height h_{AS} and BS at an height h_{BS}. The direct line-of-sight (LoS) and horizontal distance from BS to AS are represented by d_{los} and d, respectively. The elevation angle with the ground plane of LoS multipath component is θ_{los}. The d_{los} and θ_{los} are expressed as,

$$d_{\text{los}} = \sqrt{d^2 + (h_{\text{AS}} - h_{\text{BS}})^2}. \tag{1}$$

$$\theta_{\text{los}} = \arctan\left(\frac{h_{\text{AS}} - h_{\text{BS}}}{d}\right). \tag{2}$$

The propagation path delay associated with longest and shortest (LoS) paths is denoted by $\tau_{\max}$ and τ_o, respectively. The sum of distance from each foci point of an ellipse to any point on its surface is always the same. Exploiting this property, the spatial limits of scattering region can be defined by the ellipsoid corresponded from the mutipath wave having longest path delay. The axis (minor and major) of ellipsoid (E_τ) can be calculated from the longest path delay ($\tau_{\max}$). The equations for calculating axis are given below,

$$a_\tau = \frac{c\ \tau_{\max}}{2}. \tag{3}$$

$$b_\tau = \sqrt{a_\tau^2 - d_{\text{los}}^2/4}. \tag{4}$$

Moreover, the intermediate axis c_τ of the bounding ellipsoid is equal to its minor axis b_τ. Usually the elevation of AS is more than the average rooftop level; therefore, the surroundings of AS are assumed as scattering free region. Whereas, the ground BS's vicinity contain dense spatial distribution of scattering structures. For this reason, the region around BS is controlled by the ellipsoid (E_τ) which is truncated by plane of height at rooftop level and the ground plane. The distribution of scatterers is assumed as uniform. These scatterers are confined inside the truncated ellipsoidal shaped scattering region (TESR). σ_b denotes the rooftop height around the BS. The PDF of AoA for such a scenario with respect to azimuth and elevation plane taken from both ends are given in [17] in the form of $p(\phi_a)$, $p(\beta_a)$, $p(\phi_b)$, and $p(\beta_b)$. The angles formed in azimuth and elevation planes with angle of signal corresponding from a point of scattering are denoted by ϕ_b and β_b at the BS and are represented by ϕ_a and β_a at the AS, respectively.

The methodology used for computing the SFs is same as used by Durgin $et\ al.$ [2] and Khan [3]. The distribution of multipath components is described by function $p(\phi)$ or $p(\beta)$ where ϕ and β are the azimuthal and elevational AoA. They used fourier coefficients or trigonometric moments for analyzing PDF of AoA. The two methods results the same but we used the approach given in [3] because it is helpful in determining the directional data and gives actual information about the physical dimensions of the SFs. This method also defined SF, angular spread, in another form as standard deviation. The same approach is also used in [11–13].

The *n*th complex trigonometric moments of any angular distribution is $\bar{R}_n$. For example, for $p(\alpha)$, (i.e., where α may be ϕ or β for the azimuthal and elevational AoA), whose total power is equal to $P_o =$

$\int_0^{2\pi} p(\alpha)\mathrm{d}\alpha$, $\bar{R}_n$ is defined as,

$$\bar{R}_n = \bar{C}_n + j\bar{S}_n \tag{5}$$

where

$$\bar{C}_n = \frac{1}{P_o}\int_0^{2\pi} p(\alpha)\ cos(n\alpha)\mathrm{d}\alpha \tag{6}$$

and

$$\bar{S}_n = \frac{1}{P_o}\int_0^{2\pi} p(\alpha)\ sin(n\alpha)\mathrm{d}\alpha. \tag{7}$$

In case of discrete data, the definition for trigonometric moments can be modified. Only first and second moments are used in characterization of the SFs. $|\bar{R}_1|$ is the magnitude of first trigonometric moment. It can take values between 0 and 1. Close to 0 value means receiver is receiving signals from a wider range of angles and close to 1 means small angular width of AoA. The SF angular spread, Λ_α, is given as below,

$$\Lambda_\alpha = \sqrt{1 - |\bar{R}_1|^2}. \tag{8}$$

The standard deviation, σ_α, gives angular energy distribution in radians which is given as,

$$\sigma_\alpha = \sqrt{-2ln(|\bar{R}_1|)}. \tag{9}$$

The other two SFs angular constriction γ_α, and orientation parameter α_{MF}, are defined by Durgin *et al.* in [2]. γ_α gives concentration of multipath about two directions and α_{MF} provides direction of maximum fading. Their relation with trignometric moments is given below,

$$\gamma_\alpha = \frac{|\bar{R}_2 - \bar{R}_1^2|}{1 - |\bar{R}_1|^2} \tag{10}$$

and

$$\alpha_{MF} = \frac{1}{2}\mathrm{phase}\{\bar{R}_2 - \bar{R}_1^2\}. \tag{11}$$

III. Results and Discussions

This section presents an analysis on results of SFs for aeronautical communication channel. The SF, angular spread Λ_α, gives the measurement of the concentration of multipaths around a single direction by using range zero to one. The azimuthal and elevational angular spread observed from AS with respect

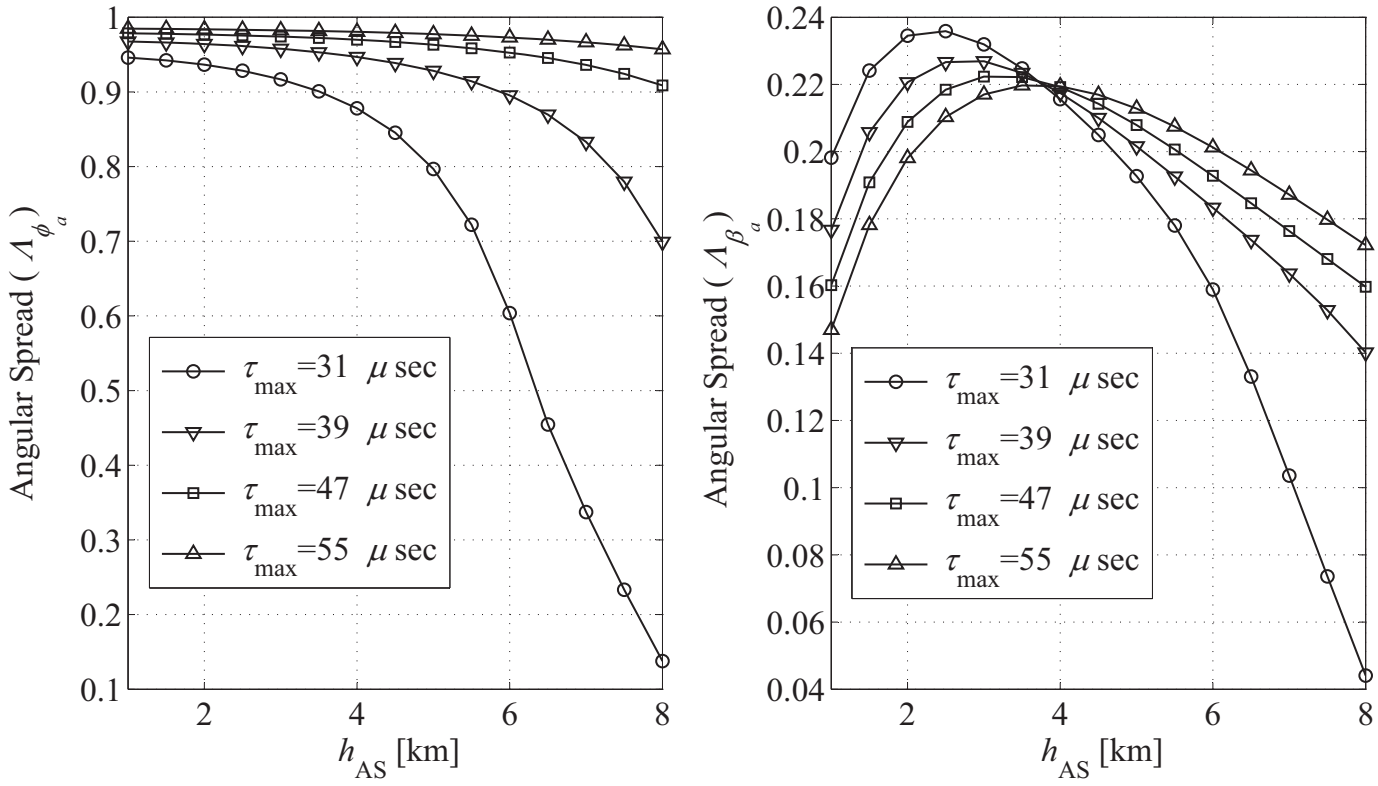

Fig. 2. Angular Spread, (a) From AS, in azimuth plane, (b) From AS, in elevation plane, ($h_{\rm BS}$ = 30m, d = 3km, and σ_b = 20m).

to height of AS for different delays of longest propagation path $(\tau_{\max})$ is shown in Fig. 2 (a) and (b), respectively. The azimuthal angular spread decreases with an increase in height of AS. However, rate of decrease increases rapidly with respect to increase in height of AS by reducing the longest path's length. The elevational angular spread observed from AS increases gradually with increase in height of AS up to an height when projection of AS lies within the scattering region but it decreases with further increase in height of AS. Moreover, the elevational angular spread shows a converse trend with respect to $\tau_{\max}$. The elevational angular spread with an increase in $\tau_{\max}$, decreases up to a certain height of AS: whereas, with further increase in height of AS, it increases.

The SF σ_α, is the standard deviation of the angular energy distribution in radians (or degrees) which gives the true physical information about the angular dispersion. The standard deviation of azimuthal and elevational distribution of angular energy observed from AS with respect to height of AS taken for different values of $\tau_{\max}$ are plotted in Fig. 3 (a) and (b), respectively. The trends for standard deviation are same as for angular spread but it gives angular spread values in degrees. Therefore it is called as another definition for angular spread giving exact true physical information for angular dispersion. The SF, angular constriction

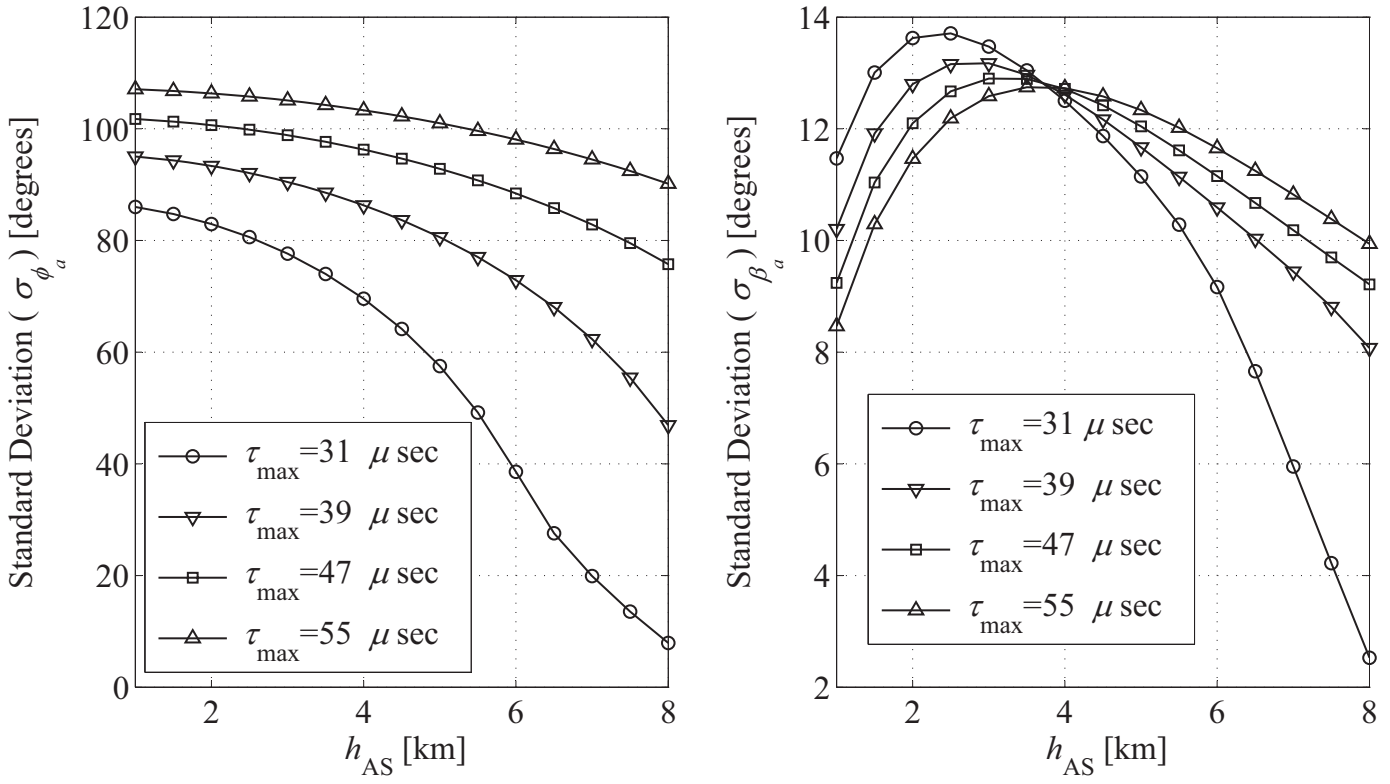

Fig. 3. Standard Deviation, (a) From AS, in azimuth plane, (b) From AS, in elevation plane,(h_{BS} = 30m, d = 3km, and σ_b = 20m).

γ_α, gives measure of concentration of multipaths around two directions. The values for γ ranges from zero to one, with one denotes arrival of exactly two multipath components from different directions and zero denotes no clear bias in two arrival directions [2]. The angular constriction for azimuth and elevation angles observed from AS with respect to height of AS is plotted in Fig. 4 (a) and (b), respectively. The angular constriction with azimuth angles increases with increase in height of AS however rate of increase is decreasing with increase in $\tau_{\max}$. The concentration around zero is evident that for a certain height AS lies with in scattering region however when AS came outside the scattering region, the angular constriction has values near one which means now multipaths are receiving from fewer directions. The angular constriction from elevation angles is gradually increasing with increase in height of AS. Moreover, with increase in $\tau_{\max}$, it decreases. The SF, α_{MF}, for these scenarios stays about -90^o.

The azimuthal and elevational angular spread observed from BS with respect to height of AS for different delays of longest propagation path is shown in Fig. 5 (a) and (b), respectively. The azimuthal angular spread is observed constant (approximately) with respect to increase in height of AS however it increases with increase in $\tau_{\max}$. An exponential increase is observed in the angular spread in elevation plane seen at BS

TABLE I. NUMERICAL VALUES OF SHAPE FACTORS FOR DIFFERENT A2G COMMUNICATION SCENARIOS

Scenarios	Angular Spread				Standard Deviation				Angular Constriction			
	Λ_{ϕ_a}	Λ_{β_a}	Λ_{ϕ_b}	Λ_{β_b}	σ_{ϕ_a}	σ_{β_a}	σ_{ϕ_b}	σ_{β_b}	γ_{ϕ_a}	γ_{β_a}	γ_{ϕ_b}	γ_{β_b}
Arrival / Take-off (h_{AS} = 1.1km, d = 2km, $\tau_{\max}$ = 7 μsec)	0.086	0.077	0.380	0.014	4.95	4.44	22.64	0.839	0.995	0.996	0.993	0.999
En-route (h_{AS} = 10km, d = 9.5km, $\tau_{\max}$ = 33 μsec)	0.165	0.129	0.062	0.002	9.63	7.47	3.79	0.147	0.971	0.976	0.970	0.999
Taxiing / Parking (h_{AS} = 0.25km, d = 0.2km, $\tau_{\max}$ = 0.7 μsec)	0.199	0.133	0.656	0.051	11.52	7.69	43.04	2.97	0.965	0.971	0.999	0.999

with increase in height of AS. Furthermore, the rate of increase in angular spread is decreases with increase in longest propagation path's length. The standard deviation of azimuthal and elevational distribution of angular energy observed from BS with respect to height of AS taken for different values of $\tau_{\max}$ are plotted in Fig. 6 (a) and (b), respectively. This definition of angular spread shows the same trends as in previous one but it is the exact measure of angular spread in degrees.

The angular constriction for azimuth and elevation angles for different values of height of BS observed from BS with respect to height of AS is plotted in Fig. 7 (a) and (b), respectively. The angular constriction remains almost constant with respect to azimuth angles with increase in height of AS as long as AS lies inside the scattering region. However it increases with increase in h_{BS}. The angular constriction with elevation angles has a gradual decrease with increase in height of AS. However, conversely with azimuthal side, it decreases with increase in h_{BS}. The SF, α_{MF}, for these scenarios remains around 0^o. As the azimuthal angular spread graphs decreases from one to zero and azimuthal angular constriction graphs increase from zero to one. It is evident that if there is not a bias in either one or two directions of AoA, then angular spread, Λ_α, will be one and angular constriction, γ_α, will be zero. The A2G communication environments are usually classified into take-off/arrival, en-route, and taxing/parking scenarios. For these scenarios, numerical results of SFs observed from both ends of the communication link are given in table I. The parameters, height of AS, distance between communicating nodes, and longest propagation path's delay; for these

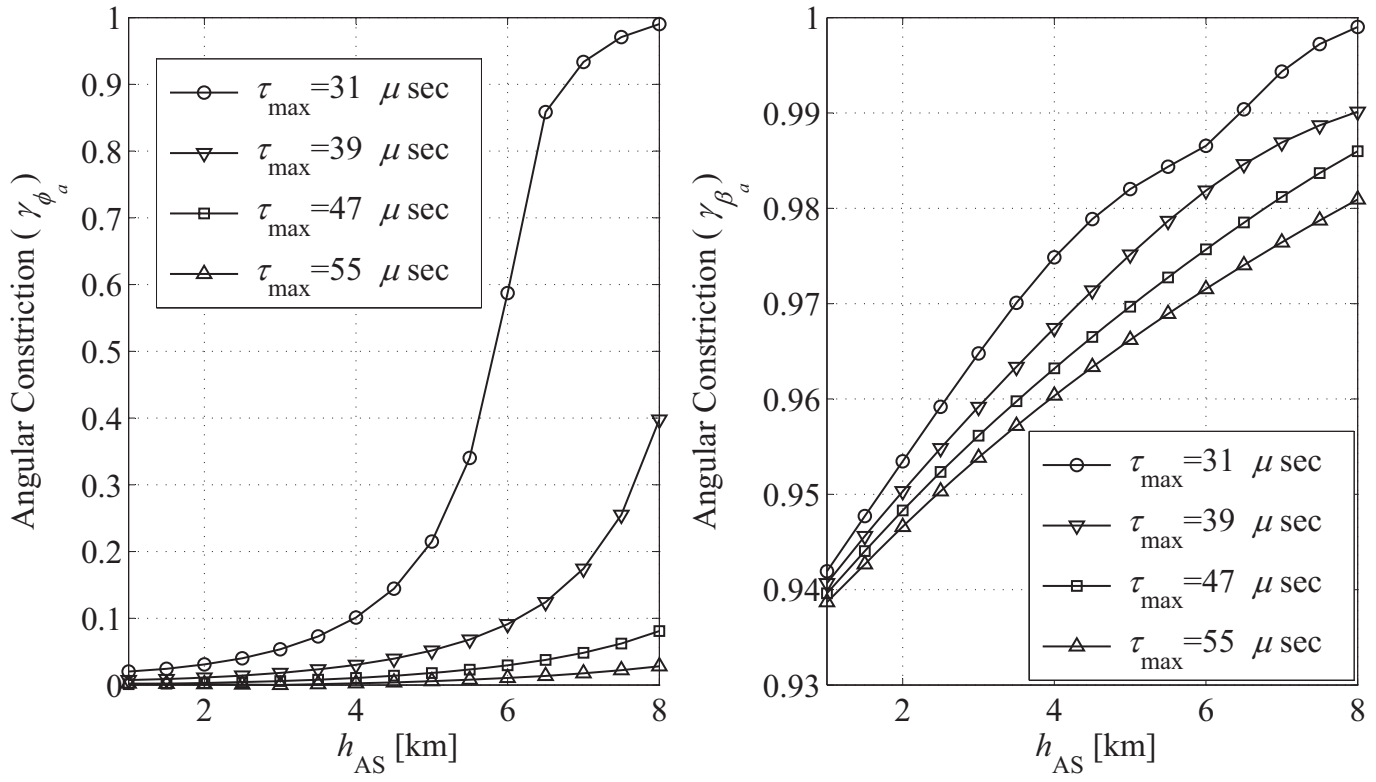

Fig. 4. Angular Constriction, (a) From AS, in azimuth plane, (b) From AS, in elevation plane, (h_{BS} = 30m, d = 3km, and σ_b = 20m).

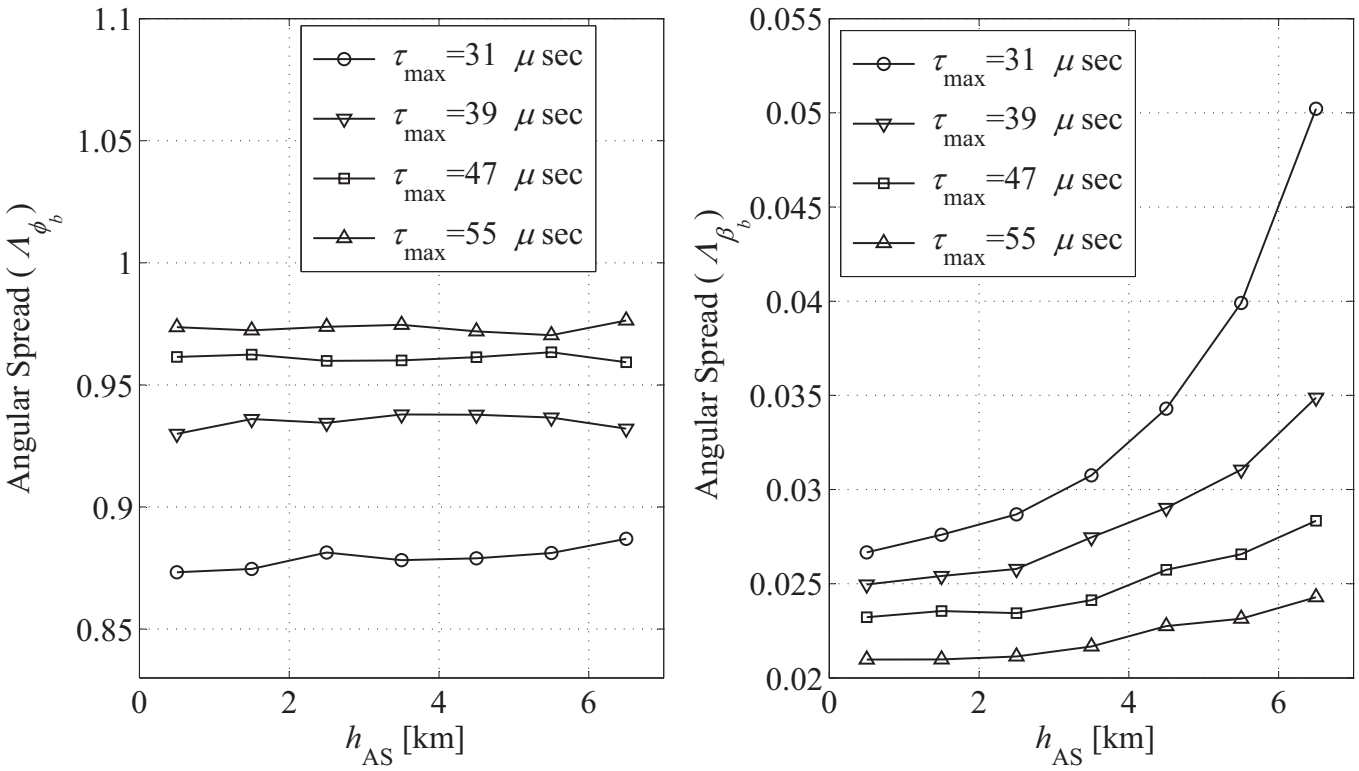

Fig. 5. Angular Spread, (a) From BS, in azimuth plane, (b) From BS, in elevation plane, (h_{BS} = 70m, d = 3km, and σ_b = 30m).

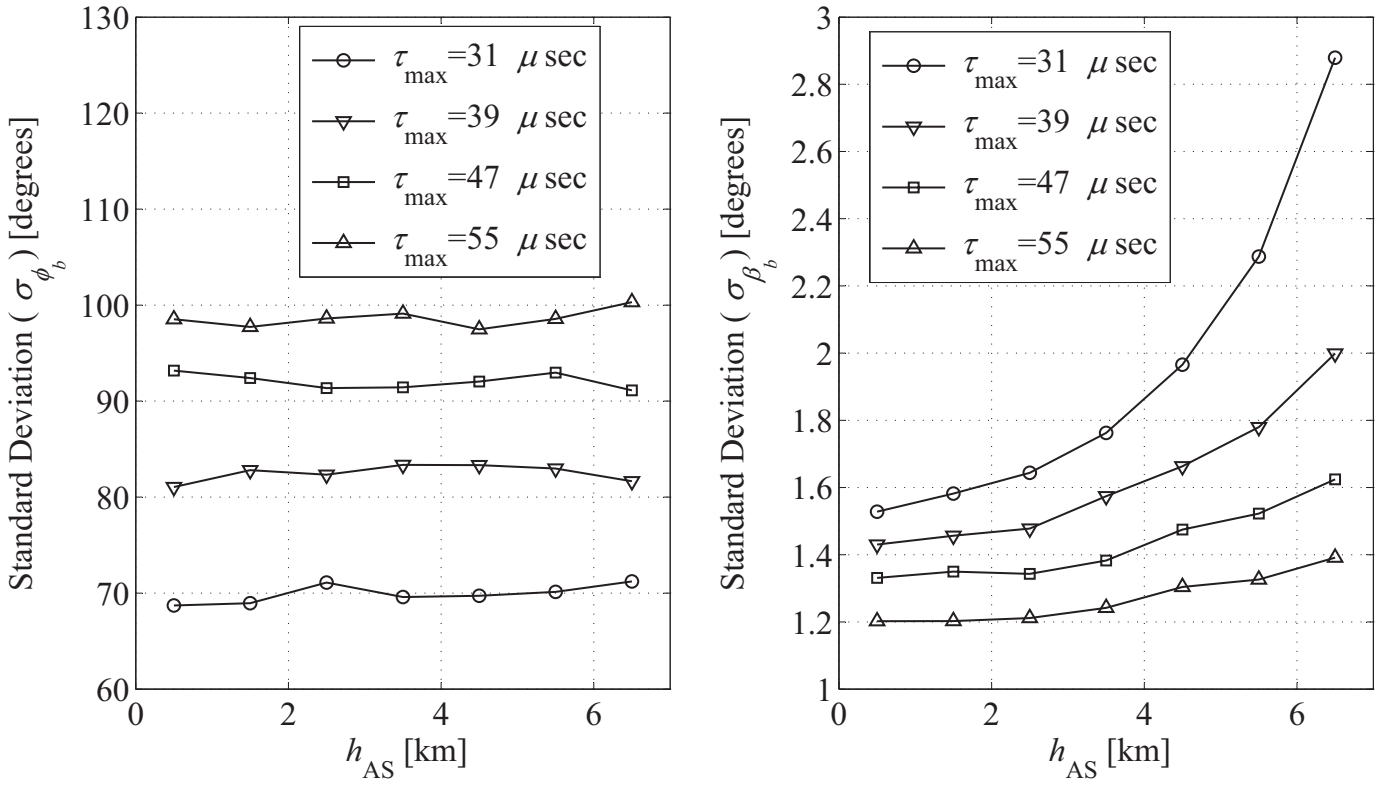

Fig. 6. Standard Deviation, (a) From BS, in azimuth plane, (b) From BS, in elevation plane, (h_{BS} = 70m, d = 3km, and σ_b = 30m).

typical propagation scenarios are taken same as measured in experimental studies given in [18, 19]. The proposed analysis on SFs for A2G/G2A communication environments are useful in studying second order fading statistics, like, level crossing rate, average fade duration, auto-covariance, and coherence distance. The proposed analysis can be used in designing beamwidth for phased antenna arrays by manipulating the correlations among antenna elements.

IV. Conclusion

An extension of a notable 3D analytical model for aeronautical communication channels, from the plain distribution of angular energy to the quantization of multipath SFs has been presented. Furthermore, an analysis on multipath SFs for A2G communication environments has been presented. The SFs are the angular spread, standard deviation, angular constriction, and direction of maximum fading. The SFs are computed using knowledge of PDFs of AoA at both ends of the communication link with respect to both elevation plane and azimuth plane. The impact of varying the height of AS, height of BS, and longest propagation path's delay on these SFs has been thoroughly observed. The SFs are analyzed numerically for different scenarios of A2G communication environment for available measured parameters.

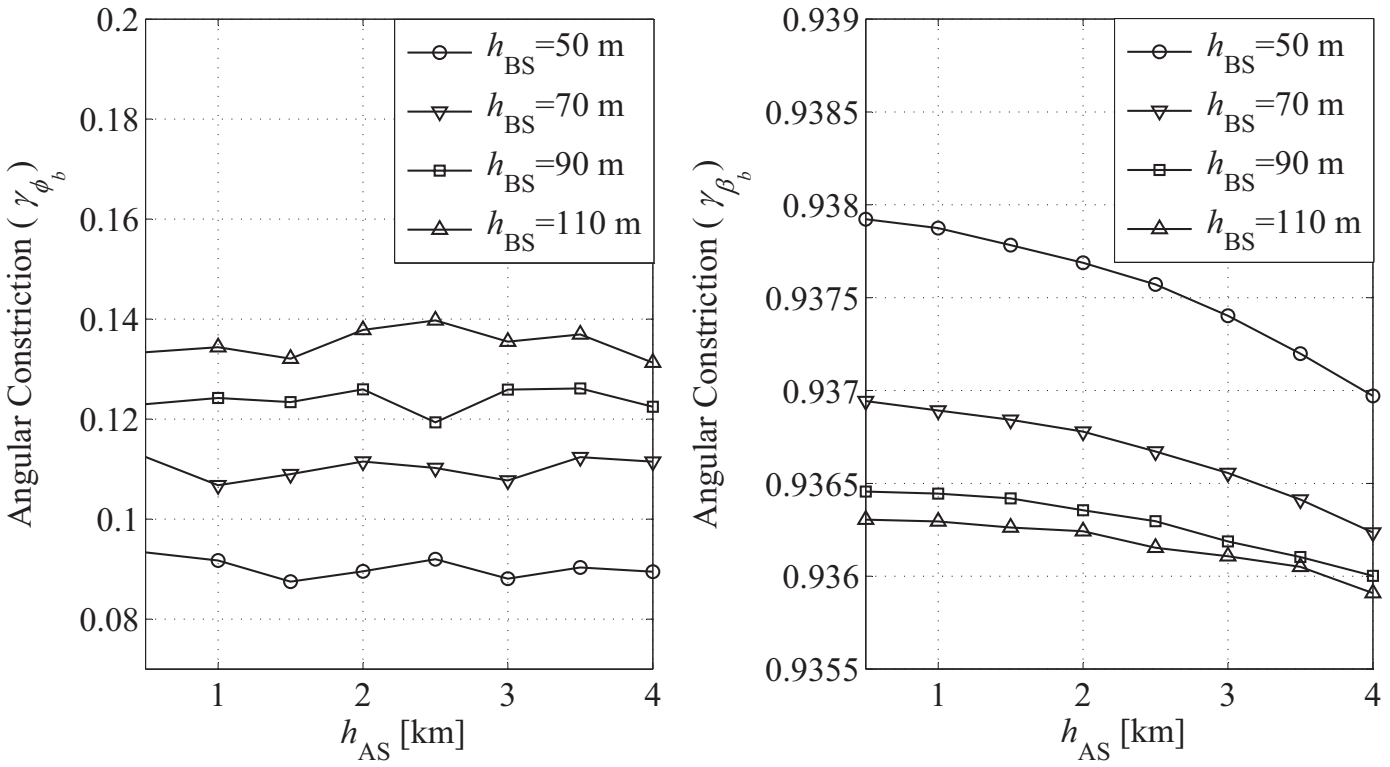

Fig. 7. Angular Constriction, (a) From BS, in azimuth plane, (b) From BS, in elevation plane, ($\tau_{\max}$ = 30 μsec, d = 3km, and σ_b = 30m).

ACKNOWLEDGMENTS

A part of this work was funded by the EU ATOM-690750 research project approved under the call H2020-MSCA-RISE-2015. The authors would also like to acknowledge the Higher Education Commission of Pakistan for a travel grant to attend this conference.

REFERENCES

[1] S. T. Rappaport, *Wireless Communications: Principles and Practice*, 2nd ed. Prentice Hall, 2002.

[2] G. D. Durgin and T. S. Rappaport, "Theory of multipath shape factors for small-scale fading wireless channels," *IEEE Trans. on Antenn. and Propag.*, vol. 48, no. 5, pp. 682–693, May 2000.

[3] N. M. Khan, "Modeling and characterization of multipath fading channels in cellular mobile communication system," Ph.D. dissertation, School of Electrical Engineering and Telecommunication, University of New South Wales (UNSW), Australia, Mar. 2006.

[4] J. Lu and Y. Han, "Application of multipath shape factors in nakagami-m fading channel," in *Proc. of Int. Conf. on Wireless Commun. Signal Processing, WCSP 2009.*, Nov. 2009, pp. 1–4.

[5] H. Y. Shang, Y. Han, and J. Lu, "Statistical analysis of rician and nakagami-m fading channel using multipath shape factors," in *Proc. of Int. Conf. on Computational Intelligence and Natural Computing (CINC) 2010.*, vol. 1, Sep. 2010, pp. 398–401.

[6] M. Alsehaili, A. Sebak, and S. Noghanian, "A 3-D geometrically based ellipsoidal wireless channel model," in *Proc. of 12th Int. Symp. on Antenn. Technol. and Applied Electromagnetics*, Jul. 2006, pp. 407–410.

[7] S. J. Nawaz, B. H. Qureshi, and N. M. Khan, "A generalized 3-D scattering model for a macrocell environment with a directional antenna at the BS," *IEEE Trans. on Veh. Technol.*, vol. 59, no. 7, pp. 3193–3204, Sep. 2010.

[8] M. Riaz, N. M. Khan, and S. J. Nawaz, "A generalized 3D scattering channel model for spatio-temporal statistics in mobile-to-mobile communication environment," *IEEE Trans. on Veh. Technol.*, vol. pp, no. 99, Nov. 2014.

[9] K. B. Baltzis and J. N. Sahalos, "A simple 3-D geometric channel model for macrocell mobile communication," *Wireless Pers. Commun.*, vol. 51, no. 2, pp. 329–347, Oct. 2009.

[10] A. Ahmed, S. J. Nawaz, and S. M. Gulfam, "A 3-D propagation model for emerging land mobile radio cellular environments," *PLoS ONE*, vol. 10, no. 8, p. e0132555, 2015.

[11] Z. M. loni and N. M. Khan, "Analysis of fading statistics in cellular mobile communication systems," *The J. of Supercomputing*, vol. 64, no. 2, pp. 295–309, 2013.

[12] Z. M. Loni, R. Ullah, and N. M. Khan, "Analysis of fading statistics based on angle of arrival measurements," in *Proc. of Int. Workshop on Antenn. Technol. (IWAT)*, Mar. 2011, pp. 314–319.

[13] Z. M. loni and N. M. Khan, "Analysis of fading statistics based on geometrical and statistical channel models," in *Proc. of Int. Conf. on Emerging Technol. (ICET)*, Oct. 2010, pp. 221–225.

[14] Y. S. Meng and Y. H. Lee, "Measurements and characterizations of air-to-ground channel over sea surface at C-band with low airborne altitudes," *IEEE Trans. on Veh. Technol.*, vol. 60, no. 4, pp. 1943–1948, May 2011.

[15] W. G. Newhall, R. Mostafa, C. Dietrich, C. R. Anderson, K. Dietze, G. Joshi, and J. H. Reed, "Wideband air-to-ground radio channel measurements using an antenna array at 2 GHz for low-altitude operations," in *Proc. of IEEE Military Commun. Conf.*, vol. 2, 2003, pp. 1422–1427.

[16] Y. S. Meng and Y. H. Lee, "Multipath characterization and fade mitigation of air-to-ground propagation channel over tropical sea surface at C band," in *Proc. of IEEE Antenn. and Propag. Society Int. Symp. (APSURSI)*, 2010, pp. 1–4.

[17] S. M. Gulfam, S. J. Nawaz, M. N. Patwary, and M. Abdel-Maguid, "On the spatial characterization of 3-D air-to-ground radio communication channels," in *Proc. of IEEE Int. Conf. on Commun. (ICC)*, Jun. 2015, pp. 2924–2930.

[18] E. Haas, "Aeronautical channel modeling," *IEEE Trans. on Veh. Technol.*, vol. 51, no. 2, pp. 254–264, Mar. 2002.

[19] G. Dyer and T. G. Gilbert, "Channel sounding measurements in the VHF A/G radio communications channel," AMCP doc., Oberpfaffenhofen, Tech. Rep. AMCP/WG-D/8-WP/19, Dec. 1997.